Human Movement Science 68 (2019) 102524

Contents lists available at ScienceDirect

Human Movement Science

journal homepage: www.elsevier.com/locate/humov

Full Length Article

The timing of locomotor propulsion in healthy adults walking at multiple speeds

Daniel Kuhman[a,*], Christopher P. Hurt[a,b]

[a] Rehabilitation Science, University of Alabama at Birmingham, Birmingham, AL, USA
[b] Department of Physical Therapy, University of Alabama at Birmingham, Birmingham, AL, USA

A B S T R A C T

In computational models of human walking, both magnitude and timing of locomotor propulsion are important for mechanical and metabolic efficiency, suggesting that these are likely tightly controlled by the neuromuscular system. Studies of actual human walking have focused primarily on magnitude-related measures of propulsion, often ignoring its timing. The purpose of this study was to quantify the timing of onset and peak propulsion relative to contralateral heel strike (HS) in healthy, young adults walking at multiple speeds. Propulsion was quantified at the ground-level using the anterior component of the anteroposterior ground reaction force, the limb-level using individual limb power, and the joint-level using ankle power. Contrary to common computational models, most of our timing-related measures indicated that propulsion occurred after contralateral HS. Timing-related measures of propulsion also changed with walking speed – as speed increased, individuals initiated propulsion earlier in the support phase. Timing of locomotor propulsion is theoretically important for walking performance, especially metabolic efficiency, and could therefore provide important clinical information. This study provides a set of relatively simple metrics that can be used to quantify propulsion and benchmark data that can be used for future comparisons with individuals or populations with gait impairments.

1. Introduction

Human walking is a complex movement that requires biological tissues (e.g., muscles, tendons) to absorb and generate energy (i.e., perform negative and positive work, respectively) throughout each gait cycle. During constant speed walking over level ground, negative work is compensated by positive work, such that the sum of the two (i.e., net work) is approximately zero across each stride. Most of this mechanical work, both positive and negative, is performed during step-to-step transitions to redirect the velocity of the CoM from a downward to an upward trajectory, effectively transitioning the CoM from one inverted pendular arc to the next (see Kuo & Donelan, 2010 for a detailed description) (Donelan, Kram, & Kuo, 2002a; Donelan, Kram, & Kuo, 2002b; Kuo, 2002, 2007; Kuo & Donelan, 2010). Principles of dynamic walking suggest that these transitions are achieved with the most mechanical efficiency by applying an impulsive push along the trailing limb ("propulsion") immediately prior to heel strike ("collision") of the leading limb (Kuo, 2002, 2007; Kuo & Donelan, 2010). Such a strategy reduces CoM vertical velocity immediately prior to HS, reducing the amount of negative work performed by the leading limb during collision, and thus lowering the amount of compensatory positive work required from the trailing limb (Kuo, 2002). If propulsion is performed too late (e.g., after HS) or too early, CoM velocity remains relatively high at collision, leading to larger collisional losses and thus lower mechanical efficiency. Indeed, computational models suggest that mistimed propulsion, whether occurring too early or too late in support, comes with negative mechanical and metabolic consequences (Kuo, 2001, 2002; Kuo & Donelan, 2010; McGeer, 1993; Ruina, Bertram, & Srinivasan, 2005). As such, timing of locomotor propulsion is likely a tightly controlled aspect of healthy gait and may be a clinically relevant biomechanical measure, as heightened metabolic cost due to mistiming could lead to fatigue and subsequently reduced physical activity or limited

* Corresponding author at: 1716 9th Ave S, Birmingham, AL 35233, USA.
E-mail address: dkuhman@uab.edu (D. Kuhman).

https://doi.org/10.1016/j.humov.2019.102524
Received 4 April 2019; Received in revised form 18 July 2019; Accepted 23 September 2019
Available online 13 November 2019
0167-9457/

community ambulation. Despite its importance for healthy gait and potential clinical usefulness, there is a surprising lack of data precisely describing the timing of locomotor propulsion during normal, human walking.

Throughout the literature describing human gait, locomotor propulsion has been captured at multiple levels. It has been quantified at the ground-level using the anterior component of the anteroposterior ground reaction force (AP GRF_{prop}), the limb-level using the positive power generated by the limb during late support, and the joint-level using the positive power generated by the ankle plantarflexors (PFs) during push-off (Browne & Franz, 2017a, 2017b; Conway, Bissette, & Franz, 2018; Zelik & Adamczyk, 2016). Decades of biomechanical research have been devoted to understanding locomotor propulsion at all three levels described above. However, much of the work on actual human walking (i.e., not model or simulation based) has focused solely on magnitude-related variables such as peak propulsive power and/or work (force and/or impulse when using AP GRF_{prop}), often ignoring its timing. For example, these magnitude-related measures have been shown to increase dramatically when the demand for locomotor propulsion is heightened. Specifically, healthy individuals increase peak AP GRF_{prop}, limb propulsive power, and ankle PF power to reach faster walking speeds, to walk uphill, and to walk against horizontally applied resistive forces (Browne & Franz, 2017b; Conway et al., 2018; Franz & Kram, 2014; Franz, Lyddon, & Kram, 2012; Lay, Hass, & Gregor, 2006; Schache, Brown, & Pandy, 2015; Winter, 1983). Less experimental work has been devoted to describing the timing of locomotor propulsion during normal human walking. Although Adamczyk and Kuo (2009) reported consistent impulse overlap of leading and trailing limb GRFs across speeds (suggesting consistent propulsion timing), the precise timing of locomotor propulsion during normal human walking is missing from the literature. (Adamczyk & Kuo, 2009).

Viewing locomotor propulsion from a joint-level perspective, as opposed to ground-level or limb-level perspectives, provides more precise information regarding the roles of individual joints and/or the muscle groups spanning those joints. As such, a joint-level perspective is likely more clinically relevant, as it provides information that could help steer interventions (e.g., assistive devices, exercise, etc.) toward more specific targets. Previous research exploring joint-level biomechanics during walking have shown that the ankle plantarflexors (PF) are largely responsible for providing locomotor propulsion, at least in healthy, young adults. Indeed, the ankle PFs provide ~40–50% of all positive work performed during the support phase of walking and the timing of this work coincides with the timing of ground- and limb-level measures of propulsion (Alexander, Strutzenberger, Ameshofer, & Schwameder, 2017; Farris & Sawicki, 2012; Zelik & Adamczyk, 2016; Zelik & Kuo, 2010). Additionally, as mentioned above, the magnitude of ankle PF power increases dramatically when the demand for locomotor propulsion is heightened (Alexander et al., 2017; Conway et al., 2018; Lay et al., 2006; Schache et al., 2015; Winter, 1983). Recent research has also found that even when walking speed is held constant, healthy adults can modify AP GRF_{prop} when given visual biofeedback and that they do this, in part, by modifying ankle PF power (Browne & Franz, 2017b). Combined, these findings indicate that healthy, young adults modulate the magnitude of locomotor propulsion largely by modulating the magnitude of mechanical power generated by the ankle PFs. Given their large role in modulating *magnitude* of propulsion, it seems likely that the ankle PFs also play a large role in modulating the *timing* of propulsion. It follows then – based on principles of dynamic walking – that to achieve the most economical gait, ankle PF power generation should be initiated, and potentially reach its peak, immediately prior to contralateral HS. Further, modifying the timing of ankle PF power should elicit metabolic changes – specifically, forcing ankle PF power to occur either too early or too late in support should raise the metabolic cost of walking. Indirect experimental evidence supports these claims. For example, altering the actuation (i.e., power onset) timing of an ankle-foot exoskeleton has been shown to alter the metabolic cost of walking in healthy adults, with optimal efficiency achieved when actuation occurs at ~37% of the stride cycle, which is, on average, just prior to contralateral HS (Malcolm, Derave, Galle, & De Clercq, 2013). These findings suggest that the ankle PFs are responsible for modulating the timing of locomotor propulsion and that the optimal timing of ankle PF power onset (and potentially peak) is immediately prior to HS of the leading limb. Surprisingly, however, there is little experimental evidence supporting or refuting that this is the case during normal human walking (i.e., non-model or non-simulation based and without external devices).

Our understanding of locomotor propulsion is fundamentally incomplete because very little is known about its precise timing, especially at the joint level, during normal human walking. Models, simulations, and prosthetic and robotic studies suggest that the timing of propulsion (at all levels) plays an important role in mechanical and metabolic efficiency during walking (Kuo, 2001, 2002, 2007; Kuo & Donelan, 2010; Malcolm et al., 2013; McGeer, 1993; Ruina et al., 2005). Measures related to the timing of propulsion may therefore be important features of gait to consider going forward, especially for clinical biomechanical analyses in populations reported to have metabolically inefficient gait patterns. An important first step is to provide descriptive data characterizing such timing-related measures in healthy, young adults. Therefore, the purpose of this study was to quantify the timing of onset and peak propulsion (at the ground-, limb-, and joint-level) in healthy, young adults walking at multiple speeds. Guided by the principles of dynamic walking, we were particularly interested in the timing of propulsion relative to HS of the leading limb. Based on those same principles, two hypotheses were formulated. First, we hypothesized that healthy, young adults would initiate and reach peak propulsion prior to HS of the leading limb. Second, we hypothesized that the timing of propulsion relative to contralateral HS would remain consistent across a range of speeds. This latter hypothesis was formed in light of the work of Adamczyk and Kuo (2009), who showed that the relative timing of propulsion and collision was consistent across a wide range of walking speeds (Adamczyk & Kuo, 2009). Precisely quantifying the timing of locomotor propulsion will not only add to our basic understanding of human gait but could also provide useful information for interventions (e.g., gait retraining, prosthetics, exoskeletons) aiming to restore or assist biological function.

2. Methods

2.1. Participants

Fifteen healthy, young adults (8 female; age = 25 ± 2; height = 1.7 ± 0.1; mass = 72.9 ± 13.5) participated in this study. To ensure that our sample represented a healthy, unimpaired population, individuals were excluded if they had suffered lower-limb injuries in the six-months prior to participation, had previous lower-limb surgery, or any cardiovascular, neurological, or orthopedic disorder that could impact gait. This study was approved by the Institutional Review Board of the University of Alabama at Birmingham and all participants provided written informed consent prior to performing the protocol.

2.2. Experimental setup

Kinematic and GRF data were collected simultaneously using 8 infrared cameras (Vicon Motion Systems, Denver, CO, USA; 100 Hz) and a dual-belt force-instrumented treadmill (Motek Link, Amsterdam, Netherlands; 1000 Hz), respectively. Vicon Nexus, Visual 3D (C-Motion Inc., Rockville, MD, USA), and laboratory software written in MATLAB (MathWorks Inc., Natick, MA, USA) were used to collect, process, and analyze data.

2.3. Protocol

Participants performed treadmill walking trials at each of the following speeds, in this order: 0.8 ms^{-1}, 1.2 ms^{-1}, 1.6 ms^{-1}, and 2.0 ms^{-1}. Trials lasted ~60-s and data were collected for the last ~20-s during each trial. For trials at 2 ms^{-1}, participants were specifically instructed to maintain a walking gait. Brief periods of rest were given between each trial.

Passive reflective markers were used to define and track movement of the upper arms, forearms, trunk, pelvis, thighs, shanks, and feet (Burnett, Campbell-Kyureghyan, Topp, & Quesada, 2015; Kadaba, Ramakrishnan, & Wootten, 1990; Kuhman, Hammond, & Hurt, 2018). Upper arms were defined and tracked by the acromion process, the lateral epicondyle of the humerus, and a single marker placed on the anterior aspect of the upper arm. Forearms were defined and tracked by the lateral epicondyle of the humerus, the styloid process of the radius, and a single marker placed mid-forearm. The trunk was defined by left/right acromion processes and left/right posterior superior iliac spines and tracked by the acromion processes, the manubrium, and the 7th cervical vertebra. The pelvis was defined and tracked by markers placed on the left/right anterior and posterior superior iliac spines. Thigh segments were defined by left/right greater trochanters and the medial/lateral femoral epicondyles and tracked using the greater trochanter, lateral femoral epicondyle, and a marker placed on the anterior aspect of the thigh. Shank segments were defined by medial/lateral femoral epicondyles and medial/lateral malleoli and tracked using lateral femoral epicondyle, lateral malleolus, and a marker placed on the anterior aspect of the shank. Feet segments were defined by medial/lateral malleoli and first/fifth metatarsophalangeal (MP) joints and tracked using markers on the first/fifth MP joints and a single marker placed on the heel.

2.4. Data analysis

Kinematic and GRF data were filtered using low-pass Butterworth filters with cut-off frequencies of 6 Hz and 12 Hz, respectively. Heel strikes (HS) and toe offs were identified in Visual 3D based on kinematic data of the feet. All measures were calculated using the support phase only. The AP GRF was split into braking (i.e., negative; AP GRF_{brake}) and propulsive (i.e., positive; AP GRF_{prop}) phases. Ankle joint power in the sagittal plane was estimated in Visual 3D using an inverse dynamics approach to calculate the joint moment and the product of the moment and angular velocity to calculate joint power. Individual limb power was calculated in MATLAB as the sum of the products of GRF and CoM velocity in vertical, anteroposterior, and mediolateral directions (Donelan et al., 2002b):

$$P_{limb} = (GRF_{vert} \times v_{CoM,vert}) + (GRF_{ap} \times v_{CoM,ap}) + (GRF_{ml} \times v_{CoM,ml})$$

Custom software written in MATLAB was used to find all magnitude-related and timing-related variables, as described below (also see Fig. 1 for a graphic representation).

Magnitude-related variables of propulsion: At the ground level, we found peak AP GRF_{prop} and quantified the impulse of AP GRF_{prop} by integrating the propulsive phase of the AP GRF curve. At the limb level, we found peak propulsion and quantified positive propulsive work by integrating the limb power curve during the propulsive phase. At the joint level, we found peak ankle PF power and quantified ankle PF positive work by integrating the positive portion of the ankle power curve. Integrations were performed with respect to time and using the trapezoidal rule. Magnitude-related variables were quantified to confirm that these increase at faster speeds, and thus capture at least some aspect of locomotor propulsion.

Timing-related variables: In most walking models, propulsion occurs instantaneously, making it relatively easy to measure its timing (onset and peak occur simultaneously). In human walking, propulsion occurs over some period of time, making it more difficult to choose timing parameters for study (e.g., timing of onset versus timing of peak). Therefore, the timing of both onset and peak propulsion at the ground, limb, and joint levels were quantified. Specifically, we found the time differences between AP GRF_{prop} onset and contralateral HS ($\Delta t_{HS\text{ - }AP\ GRF\ onset}$), between peak AP GRF_{prop} and contralateral HS ($\Delta t_{HS\text{ - }AP\ GRF\ peak}$), and between trailing limb peak AP GRF_{prop} and leading limb peak AP GRF_{brake} ($\Delta t_{brake - prop}$). At the limb level, we found time differences between limb power propulsion onset and contralateral HS ($\Delta t_{HS - limb\ pwr\ onset}$) and between peak limb propulsive power and contralateral HS ($\Delta t_{HS - limb\ pwr\ peak}$). At the joint level, we found the time differences between ankle PF power generation onset and contralateral HS ($\Delta t_{HS -}$

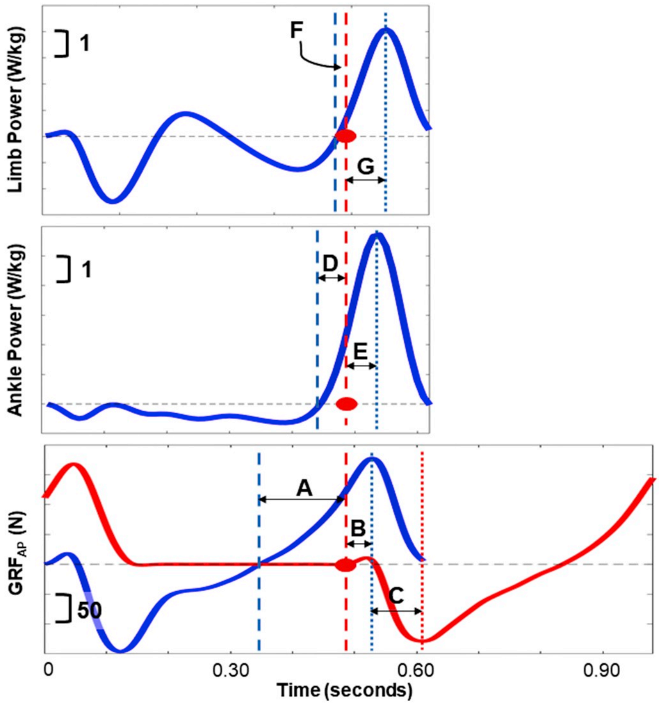

Fig. 1. Overview of the methods used to calculate timing-related variables. These are not real data. A: time difference between contralateral HS (red circle and red dashed vertical line in all graphs) and AP GRF_{prop} onset (blue dashed vertical line in bottom graph). B: time difference between contralateral HS and peak AP GRF_{prop} (blue dotted vertical line in bottom graph). C: time difference between peak trailing limb AP GRF_{prop} and peak leading limb AP GRF_{brake} (red dotted vertical line in bottom graph). D: time difference between contralateral HS and ankle PF power generation onset (blue dashed vertical line in middle graph). E: time difference between contralateral HS and peak ankle PF power (blue dotted vertical line in middle graph). F: time difference between contralateral HS and the onset of the limb power propulsive phase (blue dashed vertical line in top graph). G: time difference between contralateral HS and peak limb propulsive power (blue dotted line in top graph). (For interpretation of the references to colour in this figure legend, the reader is referred to the web version of this article.)

$_{\text{ankle pwr onset}}$) and between peak ankle PF power and contralateral HS ($\Delta t_{\text{HS − ankle pwr peak}}$). All timing variables (with one exception) were computed such that negative values indicated that onset or peak occurred after HS and positive values indicated that they occurred before HS. The only exception to this rule was $\Delta t_{\text{brake − prop}}$, which was set relative to peak braking such that negative values indicated peak propulsion occurred after peak braking and positive values indicated peak propulsion occurred before peak braking. Finally, we quantified timing of contralateral HS, AP GRF_{prop} onset and peak, limb propulsive power onset and peak, and ankle PF power onset and peak as percentages of the support phase (i.e., the percent of the support phase at which these events occurred).

For each participant, outcomes were computed for 10 strides from each leg and averaged bilaterally in each condition. Means and standard deviations in each condition across all participants are reported.

2.5. Statistical analysis

Our first hypothesis was descriptive in nature, involving simple visual inspection of the data to determine whether our measures of propulsion occurred before or after contralateral HS. To address our second hypothesis, a one-way analysis of variance (ANOVA) was used to determine the effect of walking speed on all magnitude-related and timing-related variables described above. If a significant effect of speed was found, pairwise comparisons were conducted with Bonferoni adjustments to account for multiple comparisons. Statistical significance was tested using $p < .05$. All statistical analyses were conducted using SPSS (IBM Corp., Armonk, NY, USA).

3. Results

3.1. Propulsion magnitude across speeds

Significant effects of speed were found for all magnitude-related variables of propulsion, justifying the use of AP GRF_{prop}, limb propulsive power, and ankle PF power as measures of locomotor propulsion (Table 1). On average, from 0.8 ms^{-1} to 2.0 ms^{-1}, peak AP GRF_{prop} increased by ~179%, AP GRF_{prop} impulse increased by ~69%, peak limb propulsive power increased by ~313%, limb propulsive work increased by ~207%, peak ankle PF power increased by ~244%, and ankle PF positive work increased by 200% (all

Table 1
Magnitude-related variables of locomotor propulsion across speeds, measured at the ground (AP GRF_{prop}), limb (limb propulsive power), and joint (ankle PF power) levels.

Magnitude-related variables		Walking speed			
		0.80 ms^{-1}	1.20 ms^{-1}	1.60 ms^{-1}	2.00 ms^{-1}
AP GRF_{prop}	Peak (N)	82.2 ± 14.6^{b,c,d}	129.0 ± 25.0^{a,c,d}	181.9 ± 34.3^{a,b,d}	229.6 ± 50.3^{a,b,c}
	Impulse (Ns)	15.9 ± 3.7^{b,c,d}	19.8 ± 4.9^{a,c,d}	24.2 ± 5.5^{a,b,d}	26.8 ± 6.8^{a,b,c}
Ankle PF Power	Peak (W/kg)	1.79 ± 0.22^{b,c,d}	3.31 ± 0.46^{a,c,d}	4.90 ± 0.71^{a,b,d}	6.16 ± 1.37^{a,b,c}
	Work (J/kg)	0.16 ± 0.03^{b,c,d}	0.27 ± 0.05^{a,c,d}	0.38 ± 0.07^{a,b,d}	0.48 ± 0.12^{a,b,c}
Limb Propulsive Power	Peak (W/kg)	1.39 ± 0.09^{b,c,d}	2.52 ± 0.23^{a,c,d}	4.07 ± 0.38^{a,b,d}	5.74 ± 0.77^{a,b,c}
	Work (J/kg)	0.14 ± 0.02^{b,c,d}	0.22 ± 0.03^{a,c,d}	0.33 ± 0.04^{a,b,d}	0.44 ± 0.07^{a,b,c}

Alphabetical superscripts represent statistically significant pairwise comparisons: ^{a} different from value at 0.8 ms^{-1}, ^{b} different from value at 1.2 ms^{-1}, ^{c} different from value at 1.6 ms^{-1}, ^{d} different from value at 2.0 ms^{-1}. All pairwise differences found using Bonferoni adjustments for multiple comparisons ($p < .05$).

$p < .001$). Pairwise comparisons revealed that each of these variables increased significantly with each increase in speed (all $p < .001$).

3.2. Relative timing of propulsion

The timing of locomotor propulsion relative to contralateral HS depended on the level of analysis (Table 2). AP GRF_{prop} onset occurred prior to contralateral HS at all four speeds tested (Fig. 2). Limb propulsive power onset occurred prior to contralateral HS only at 2.0 ms^{-1} (Fig. 3). Ankle PF power onset occurred prior to contralateral HS at 1.6 ms^{-1} and 2.0 ms^{-1} (Fig. 4). Peak AP GRF_{prop}, peak limb propulsive power, and peak ankle PF power occurred after contralateral HS at all four speeds tested.

When using propulsion *onset* to quantify timing-related variables of propulsion, significant effects of speed were observed at all three levels of analysis (ground, limb, joint). As walking speed increased, $\Delta t_{HS\text{ - AP GRF onset}}$ became more positive, indicating that AP GRF_{prop} onset occurred further before contralateral HS at faster speeds ($p = .001$). This change appeared to be driven by contralateral HS occurring later in support (72 ± 0.9% at 0.8 ms^{-1} to 78 ± 0.9% at 2.0 ms^{-1}; speed effect, $p < .001$) and AP GRF_{prop} beginning earlier in support (57 ± 2.9% at 0.8 ms^{-1} to 53 ± 4.6 at 2.0 ms^{-1}, $p < .001$). As walking speed increased, $\Delta t_{HS\text{ – limb pwr onset}}$ became more positive ($p < .001$) and switched from negative values at the three slower speeds to a positive value at the fastest speed. This change was driven by contralateral HS occurring later in support and limb propulsive power onset occurring slightly earlier in support (79 ± 1.3% at 0.8 ms^{-1} to 77 ± 1.9% at 2.0 ms^{-1}, $p < .001$). As walking speed increased, $\Delta t_{HS\text{ – ankle pwr onset}}$ became more positive ($p < .001$) and switched from negative values at the two slower speeds to positive values at the two faster speeds. This change was driven by contralateral HS occurring later in support and ankle PF power onset occurring earlier in support (79 ± 2.8% at 0.8 ms^{-1} to 70 ± 6.2% at 2.0 ms^{-1}, $p < .001$).

When using propulsion *peak* to quantify timing-related variables of propulsion, significant effects of speed were observed at all

Table 2
Timing-related variables of locomotor propulsion across speeds, measured at the ground (AP GRF_{prop}), limb (limb propulsive power), and joint (ankle PF power) levels.

Timing-related variables		Walking speed			
		0.80 ms^{-1}	1.20 ms^{-1}	1.60 ms^{-1}	2.00 ms^{-1}
	Contralateral HS (% support)	71.7 ± 0.9^{b,c,d}	74.4 ± 0.9^{a,c,d}	76.7 ± 1.0^{a,b,d}	78.5 ± 0.9^{a,b,c}
AP GRF_{prop}	Contralateral HS - AP GRF_{prop} Onset (*sec.*)	0.13 ± 0.02	0.13 ± 0.02^{d}	0.14 ± 0.01^{d}	0.15 ± 0.02^{b,c}
	Propulsive GRF Onset (% support)	57.5 ± 3.0^{d}	57.4 ± 2.9^{c,d}	56.0 ± 3.1^{b,d}	53.2 ± 4.6^{a,b,c}
	Contralateral HS - Peak AP GRF_{prop} (sec.)	−0.12 ± 0.01^{b,c,d}	−0.08 ± 0.01^{a,c,d}	−0.06 ± 0.01^{a,b,d}	−0.04 ± 0.01^{a,b,c}
	Peak Propulsive GRF (% support)	86.2 ± 1.5	86.7 ± 1.0	86.8 ± 0.7	86.7 ± 0.7
	Peak AP GRF_{brake} - Peak AP GRF_{prop} (sec.)	0.08 ± 0.03	0.08 ± 0.01	0.08 ± 0.01	0.08 ± 0.01
Ankle PF Power	Contralateral HS - Ankle Power Onset (sec.)	−0.07 ± 0.03^{b,c,d}	−0.03 ± 0.02^{a,c,d}	0.01 ± 0.03^{a,b,d}	0.05 ± 0.04^{a,b,c}
	Ankle Power Onset (% support)	79.3 ± 2.8^{c,d}	77.8 ± 2.2^{c,d}	75.2 ± 4.0^{a,b,d}	70.4 ± 6.3^{a,b,c}
	Contralateral HS - Peak Ankle Power (sec.)	−0.15 ± 0.02^{b,c,d}	−0.10 ± 0.01^{a,c,d}	−0.07 ± 0.01^{a,b,d}	−0.04 ± 0.01^{a,b,c}
	Peak Ankle Power (% support)	88.8 ± 1.2^{b,c,d}	87.9 ± 0.9^{a,c,d}	87.2 ± 0.7^{a,b,d}	85.9 ± 1.5^{a,b,c}
Limb Propulsive Power	Contralateral HS - Limb Power Onset (sec.)	−0.06 ± 0.01^{b,c,d}	−0.03 ± 0.01^{a,c,d}	−0.01 ± 0.01^{a,b,d}	0.01 ± 0.01^{a,b,c}
	Limb Power Propulsion Onset (% support)	78.9 ± 1.3^{c,d}	78.4 ± 1.3^{c,d}	77.6 ± 1.2^{a,b,d}	76.6 ± 1.9^{a,b,c}
	Contralateral HS - Peak Limb Propulsion Power (sec.)	−0.16 ± 0.01^{b,c,d}	−0.12 ± 0.01^{a,c,d}	−0.09 ± 0.01^{a,b,d}	−0.07 ± 0.01^{a,b,c}
	Peak Limb Propulsion Power (% support)	88.3 ± 1.0^{b,c}	88.8 ± 0.9^{a}	89.0 ± 0.7^{a}	89.0 ± 0.7

Alphabetical superscripts represent statistically significant pairwise comparisons: ^{a} different from value at 0.8 ms^{-1}, ^{b} different from value at 1.2 ms^{-1}, ^{c} different from value at 1.6 ms^{-1}, ^{d} different from value at 2.0 ms^{-1}. All pairwise differences found using Bonferoni adjustments for multiple comparisons ($p < .05$).

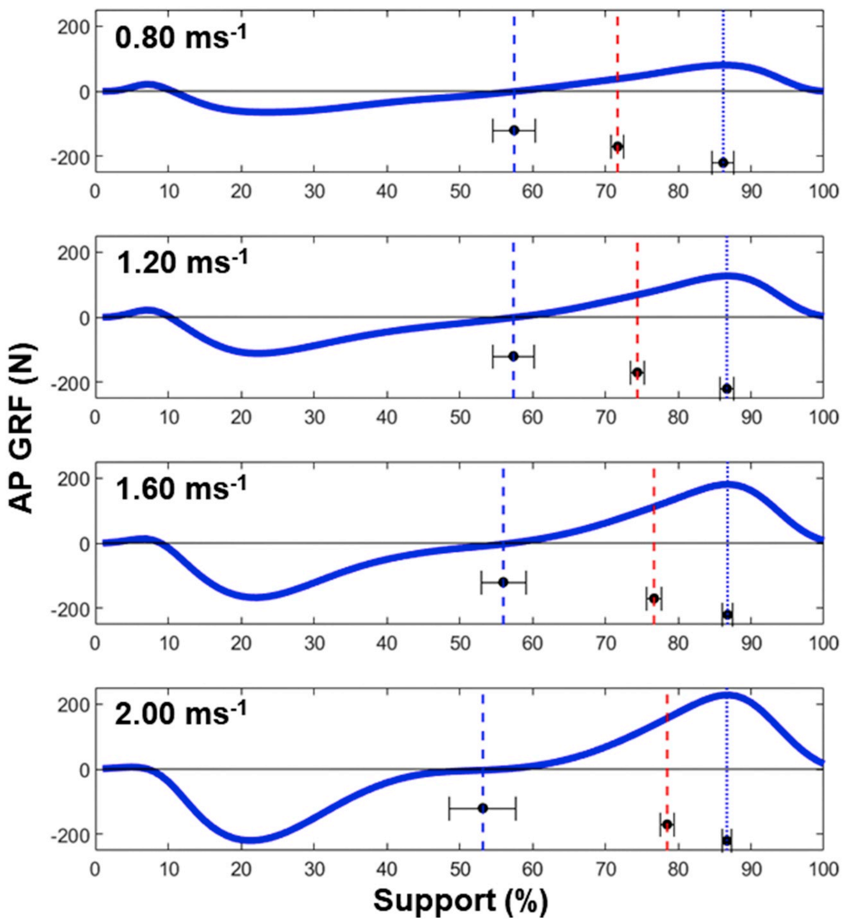

Fig. 2. Ensemble support phase AP GRF curves for all speeds. Blue dashed vertical lines represent mean timing of AP GRF_{prop} onset. Blue dotted vertical lines represent mean timing of peak AP GRF_{prop}. Red dashed vertical lines represent mean timing of contralateral heel strike. Black circles and horizontal lines laid over vertical lines represent mean ± 1 standard deviation for the timing of each event. (For interpretation of the references to colour in this figure legend, the reader is referred to the web version of this article.)

three levels of analysis (ground, limb, joint). As walking speed increased, $\Delta t_{HS\text{ - AP GRF peak}}$, $\Delta t_{HS\text{ – ankle pwr peak}}$, and $\Delta t_{HS\text{ – limb pwr peak}}$ became less negative (all $p < .001$), indicating that peak propulsion got increasingly closer to HS. The ground-level changes were apparently driven entirely by contralateral HS occurring later in support, as peak AP GRF_{prop} remained at ~86% of support at all speeds tested (non-significant speed effect, $p = .070$). The limb-level changes also appeared to be driven primarily by contralateral HS occurring later in support, as peak limb propulsive power remained at ~89% of support across speeds (however, despite only very small changes, there was a significant effect of speed on the timing of peak propulsive power, $p < .001$). The joint-level changes were driven by both contralateral HS occurring later in support and peak ankle PF power occurring slightly earlier in support (89 ± 1.2% at 0.8 ms^{-1} to 86 ± 1.5% at 2.0 ms^{-1}, $p < .001$). Finally, $\Delta t_{brake\text{ – }prop}$ did not change with walking speed ($p = .533$), indicating consistent time differences between leading limb peak AP GRF_{brake} and trailing limb peak AP GRF_{prop} (~0.08s) across all four speeds.

4. Discussion

The purpose of this study was to quantify the timing of onset and peak propulsion (at the ground, limb, and joint levels) in healthy, young adults walking at multiple speeds. Guided by principles of dynamic walking (Kuo, 2001, 2002, 2007; Kuo & Donelan, 2010), we were particularly interested in the timing of propulsion relative to contralateral HS. We hypothesized that propulsion onset and peak (as measured at all levels) would occur prior to contralateral HS. In partial support of this hypothesis, and in support of dynamic walking principles, ground-level propulsion (AP GRF_{prop}) onset occurred prior to contralateral HS at all speeds tested. However, limb-level propulsion onset occurred prior to HS only during the fastest speed tested and joint-level propulsion (ankle PF power) onset occurred prior to HS only during the fastest two speeds. Additionally, ground-, limb-, and joint-level measures of peak propulsion occurred after HS at all speeds. We also hypothesized that the timing of propulsion relative to contralateral HS would remain consistent across a range of walking speeds. This hypothesis was fully rejected, as walking speed influenced the timing of

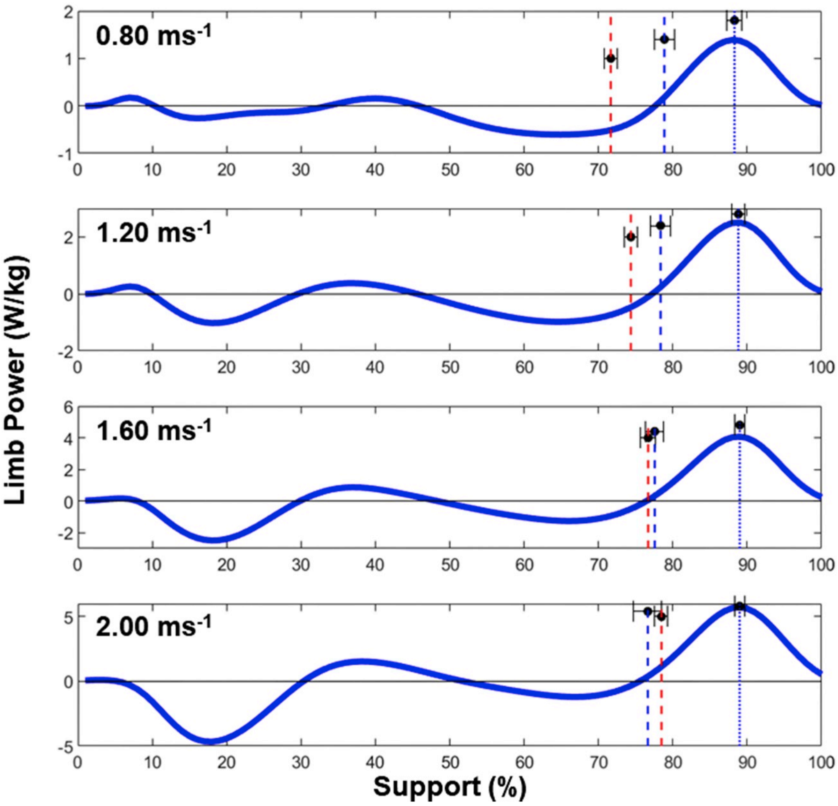

Fig. 3. Ensemble support phase limb power curves for all speeds. Blue dashed vertical lines represent mean timing of limb power propulsion onset. Blue dotted vertical lines represent mean timing of peak limb propulsive power. Red dashed vertical lines represent mean timing of contralateral heel strike. Black circles and horizontal lines laid over vertical lines represent mean ± 1 standard deviation for the timing of each event. (For interpretation of the references to colour in this figure legend, the reader is referred to the web version of this article.)

ground-, limb-, and joint-level propulsion onset and peak relative to contralateral HS. To our knowledge, this study is the first to precisely quantify the timing of locomotor propulsion during normal human walking across multiple speeds.

On average, the onset of AP GRF_{prop} occurred at ~55% of the support phase across all speeds tested, well before contralateral HS and interestingly, at a time when hip, knee, and ankle joint powers are all negative (Fig. A1). Thus, although the timing of this propulsive measure fits nicely into the dynamic walking model in that it occurs prior to HS, the origins of the measure do not. Specifically, the onset of AP GRF_{prop} does not appear to be the result of an active force applied along the limb from muscles of the lower extremity (especially from muscles spanning the ankle), as described by principles of dynamic walking. Rather, it is likely the result of the body's CoM beginning its downward trajectory and moving in front of the supporting foot (which also appears to occur at ~55–60% of support). Although magnitude-related measures of AP GRF_{prop} have been linked to important metrics of gait performance (e.g., walking speed), our timing-related results call into question whether researchers (or clinicians) should use the AP GRF as a true measure of locomotor propulsion as it relates to step-to-step transition mechanics (Browne & Franz, 2017b; Hurt, Burgess, & Brown, 2015; Nilsson & Thorstensson, 1989). Impulse of the AP GRF_{prop} is especially questionable given that some amount of this force appears to be the result of passive CoM motion. Additionally, the AP GRF does not capture the vertical component of propulsion (i.e., redirecting CoM velocity from downward to upward). It is possible that timing of some component of the vertical GRF more closely follows the principles of dynamic walking and may provide a more accurate measure of locomotor propulsion. The vertical GRF is typically bimodal, with a peak during early support, a depression during mid-support, and a second peak during late support. Although not measured here, the onset of the rise to the second peak and/or the peak itself may provide measures that more accurately capture the timing of propulsion. It is also possible that the 3-dimensional resultant GRF provides a more accurate measure of locomotor propulsion. Lending some support to this, Adamczyk and Kuo (2009) used an overlap parameter describing the simultaneity of 3-dimensional GRF impulses of trailing and leading limbs during step-to-step transitions to show that push-off consistently occurred before collision across a range of walking speeds (Adamczyk & Kuo, 2009).

Limb- and joint-level measures of locomotor propulsion employed here were likely more indicative of active modes of propulsion than our ground-level measure (for reasons described above) and are thus likely truer tests of our first hypothesis. Surprisingly, the onset of limb- and joint-level propulsion occurred after contralateral HS at most of the speeds tested, suggesting that our participants did not adhere to principles of dynamic walking, especially at speeds slower than 1.6 ms^{-1}. The dynamic walking model predicts that the highest mechanical and metabolic efficiency is achieved with pre-HS propulsion (Adamczyk & Kuo, 2009; Kuo, 2001, 2002, 2007;

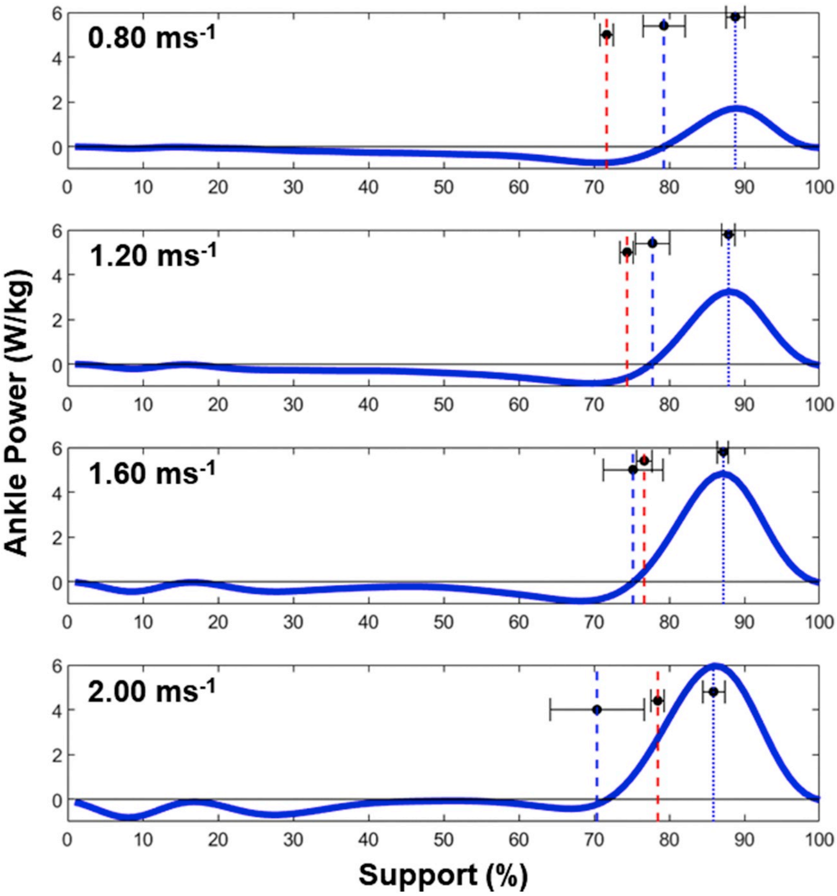

Fig. 4. Ensemble support phase ankle power curves for all speeds. Blue dashed vertical lines represent mean timing of ankle PF power generation onset. Blue dotted vertical lines represent mean timing of peak ankle PF power. Red dashed vertical lines represent mean timing of contralateral heel strike. Black circles and horizontal lines laid over vertical lines represent mean ± 1 standard deviation for the timing of each event. (For interpretation of the references to colour in this figure legend, the reader is referred to the web version of this article.)

Kuo & Donelan, 2010). Although metabolic efficiency is an important measure of gait performance and therefore a major determinant of gait mechanics, other factors (e.g., dynamic stability, maneuverability) are also important. It is possible that post-HS propulsion is a mechanism that ensures such factors, potentially at the cost of mechanical and metabolic efficiency that hypothetically results from pre-HS propulsion. However, individuals in this study walked on a treadmill at constant speeds and without perturbation, likely reducing the demand for mechanisms governing dynamic stability and maneuverability. In this environment then, it should be assumed that healthy, young adults adopt a gait pattern that optimizes metabolic efficiency and should therefore initiate propulsion prior to HS. Thus, it remains unclear why participants in this study consistently initiated ankle and limb propulsion after contralateral HS, especially at speeds slower than 1.6 ms^{-1}. Further, visual inspection of the timing of contralateral HS and propulsion relative to CoM velocity (Fig. 5) suggests that some mechanism not measured here was responsible for the vertical redirection of CoM velocity. It should be noted that in the current study, metabolic efficiency, dynamic stability, or any other measure of gait performance were not quantified. It is therefore unclear whether timing-related measures of locomotor propulsion meaningfully relate to these or other metrics of gait performance. However, correlation analyses between relative timing of onset of limb-level propulsion and collisional losses (negative work from the leading limb) at all speeds did not produce significant relationships, suggesting that between-participant variation in timing was not related to variation in collisional loss (Fig. B1).

Based on the consistent overlap of propulsive and braking GRFs (measured 3-dimensionally) reported by Adamczyk and Kuo (2009), we hypothesized that timing of propulsion relative to contralateral HS would not change across walking speeds (Adamczyk & Kuo, 2009). Our results did not support this hypothesis, as nearly all timing-related measures quantified here changed with walking speed. To determine what drove these changes, the percentages of support at which each event occurred were quantified. In general, as walking speed increased, contralateral HS occurred later in support and measures of propulsion (both onset and peak) occurred earlier in support, leading to timing-related measures becoming more positive as walking speed increased. An unplanned but nonetheless interesting observation was that the timing of peak propulsion varied less across speeds than the timing of propulsion onset, suggesting that the nervous systems maintains tighter control over the timing of peak propulsion. Our across-speed analysis also revealed that the two measures not influenced by walking speed were the percent of support at which peak AP GRF_{prop} occurred

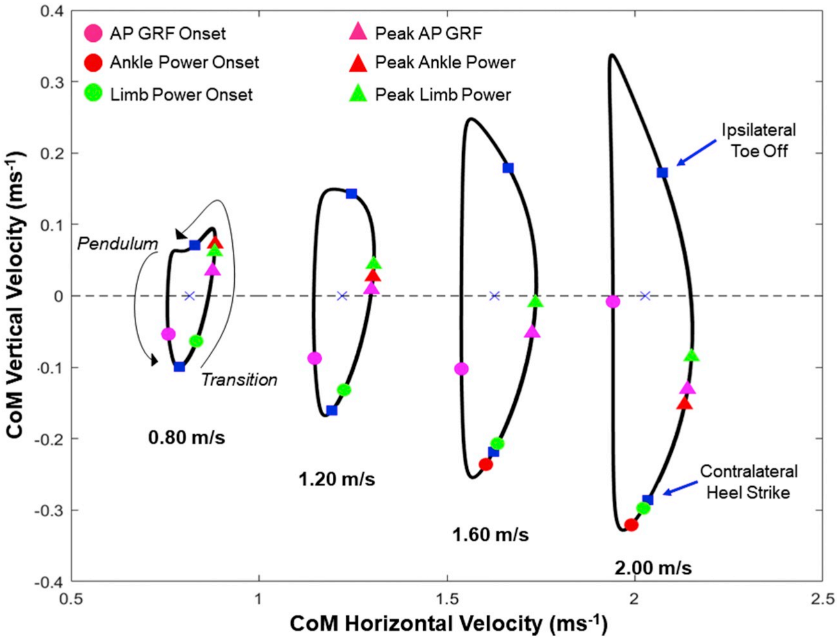

Fig. 5. Center of mass (CoM) vertical velocity plotted against CoM horizontal velocity (known as a hodograph). The minimum y-axis value of each hodograph represents the point at which the CoM is redirected from downward and forward to upward and forward (i.e., the start of the step-to-step transition). With the exception of AP GRF propulsion onset, all of our measures of propulsion onset and peak occurred after the CoM had been redirected forward and upward (i.e., after the y-axis minimum) – even those that occurred prior to contralateral heel strike.

and the time difference between lead limb peak AP GRF_{brake} and trailing limb peak AP GRF_{prop}. On average (across participants), peak AP GRF_{prop} occurred at 86% of support and 0.08s before lead limb peak AP GRF_{brake} at all walking speeds. The consistency of these two measures suggests that they may be tightly controlled by the nervous system. The invariance in time difference between peaks across speeds are predicted, in part, by the dynamic walking models and could make gait more efficient (i.e., peak-to-peak time is tightly controlled to optimize efficiency). This may also simply be a mechanical consequence of a symmetric heel-toe walking pattern. The current study was not designed to test this and, without the benefit of a controlled experiment wherein these variables are independently manipulated, clear conclusions cannot be drawn. Further studies are warranted to determine potential causes and consequences of the consistency in timing between leading and trailing limb peak AP GRFs.

Although this study included only healthy individuals, it is important to consider the potential clinical utility of our findings. As stated throughout, the timing of locomotor propulsion is likely an important factor for gait efficiency. As such, mistimed propulsion may contribute to inefficiencies reported in various clinical populations (e.g., advanced age, post-stroke, Parkinson's disease) (Christiansen, Schenkman, McFann, Wolfe, & Kohrt, 2009; Kramer, Johnson, Bernhardt, & Cumming, 2016; Mian, Thom, Ardigò, Narici, & Minetti, 2006). The results from this study provide benchmark data that can be used in future comparisons with individuals in such populations, as criteria for diagnosing abnormal propulsive timing, and as targets for interventions aiming to improve gait performance. Interventions targeting muscle force generating capacity via strength and power training are commonly administered to individuals with gait impairment (Beijersbergen et al., 2016; Brandon, Boyette, Gaasch, & Lloyd, 2000; Kim, Eng, MacIntyre, & Dawson, 2001). Future interventions incorporating timing-related components (e.g., through use of biofeedback) may help translate gains in muscular strength and power to gait performance. Indeed, Kuo and Donelan (2010) suggested nearly a decade ago that rehabilitative strategies target the timing as well as the magnitude of force generation during walking (Kuo & Donelan, 2010). Our results also provide information that could aid in the design of assistive devices. For example, post-HS propulsion onset may simplify interventions involving prosthetics or exoskeletal devices. Specifically, actuation timing of such devices on the trailing limb could be triggered by a heel switch on the leading limb. Creating a pre-HS actuation trigger may be more challenging, as it requires a time prediction of an impending event rather than using a known time from an event that has already occurred. Another previously explored alternative is to actuate a device at a pre-set percentage of the gait cycle (Malcolm et al., 2013; Malcolm, Quesada, Caputo, & Collins, 2015). This method presents its own complications, however, as it assumes that other important gait events (e.g., contralateral HS) will occur at the same time of every cycle and that step time will remain consistent across many steps. Thus, small but natural deviations in kinematics across many steps could alter device actuation timing relative to the events they are meant to precede by an exact, specified amount of time. Although variation in HS timing across steps in each condition was not quantified here, there was a significant effect of walking speed on the percent of support at which HS occurred. These results suggest that devices using pre-set actuation times would, at the very least, need to be adjusted based on the speed of the user, which itself varies greatly during community ambulation. Although post-HS propulsion would simplify these design complications, it might come at the cost of reduced mechanical and metabolic efficiency (as discussed throughout). This highlights the importance of future work quantifying the relationships between propulsion timing and metrics of walking performance.

There are several important limitations to consider when interpreting our results. Trials were performed on a treadmill, which may alter gait compared to over ground walking. Although GRFs and joint-level kinematics and kinetics are similar between treadmill and over ground walking, between-method differences in the timing-related variables reported here have not been performed (Riley, Paolini, Della Croce, Paylo, & Kerrigan, 2007). Walking trials were not randomized, which may have influenced the results. However, the protocol did not include excessively strenuous or abnormal conditions and none of the participants expressed difficulty completing any of the trials. Additionally, participants received resting periods after each trial and were allowed ≥ 40s of walking at each speed prior to data collection. The principles of dynamic walking upon which we formed our hypotheses suggest that optimal efficiency is achieved when propulsion occurs immediately prior to contralateral heel strike. It was assumed that the natural gait patterns adopted by our healthy, young participants represented optimal efficiency. However, metabolic data were not collected to confirm or refute this assumption. Relatedly, it is possible that our walking trials were not long enough for participants to reach an optimally efficient gait pattern. Finally, given the small timing differences observed in some conditions (e.g., $\Delta t_{HS\,-\,limb\ pwr\ onset}$ at 1.6 and 2 ms^{-1}), it is important to consider factors that may have limited our ability to precisely identify events and therefore to precisely quantify these timing-related measures. Such factors include data filtering techniques (which may unintentionally remove non-noise data), data sampling frequency (which determines the precision with which gait events can be identified), and methods for identify key events (e.g., using kinematic or GRF data to identify HS and TO).

5. Conclusion

Our results indicated that limb- and joint-level locomotor propulsion occurred after contralateral HS, especially at slower speeds. Additionally, the timing of locomotor propulsion relative to contralateral HS was altered with walking speed. These findings offer a more complete biomechanical description of locomotor propulsion in healthy individuals and provide a new set of potentially clinically useful parameters.

Declaration of Competing Interest

None of the authors had any competing interests related to this project.

Acknowledgements

We thank Andrew T. Baumann, Wei H. Jiang, and Kathrynne G. Marsh for their aid in participant recruitment and data collection.

Appendix A

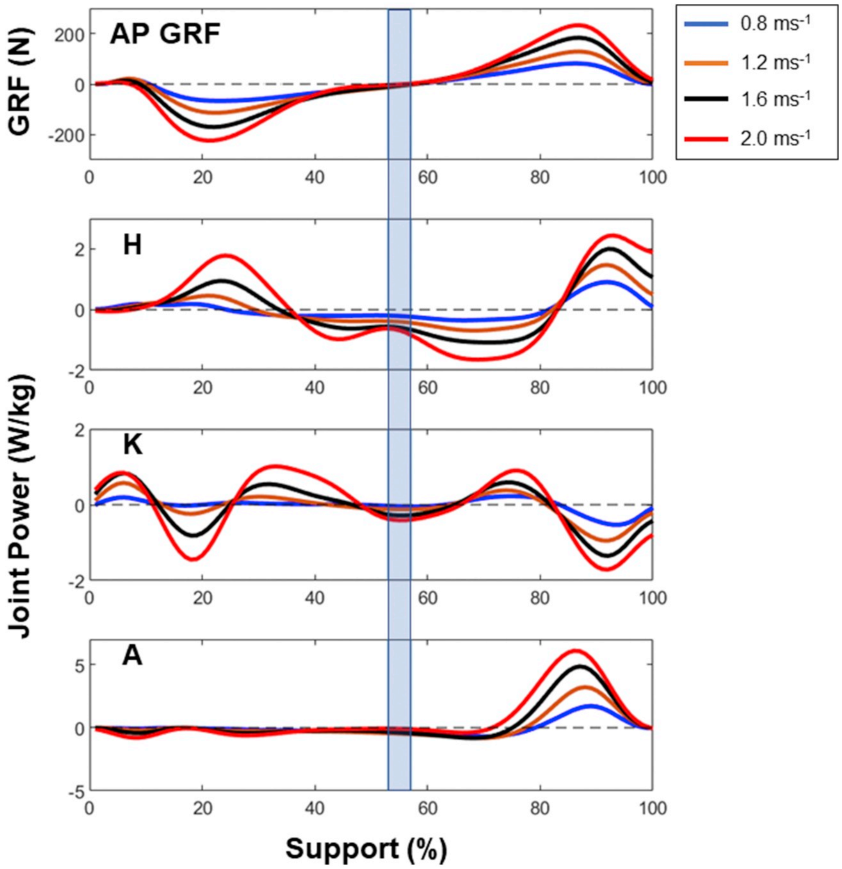

Fig. A1. Anteroposterior ground reaction force (AP GRF) and hip (H), knee (K), and ankle (A) joint powers across all speeds. The vertical blue band represents the range of time within the support phase that AP GRF turned from negative to positive across speeds. The right boundary of the band is at 57% of support and the left boundary is at 53% of support, which represent the group means for AP GRF_{prop} onset time at 0.8 and 2.0 ms^{-1}, respectively. At the two intermediate speeds, AP GRF_{prop} onset occurred at 57% and 56% (1.2 and 1.6 ms^{-1}, respectively). Interestingly, AP GRF becomes positive during a period of the support phase when power at all three joints is negative. This suggests that the initial aspect of the AP GRF may be the result of relatively passive center of mass motion rather than active muscular force. Because of this, we call into question the use of the positive aspect of the AP GRF to measure locomotor propulsion. Especially questionable is the positive impulse of AP GRF, as this will include periods which appear to be passive.

Appendix B

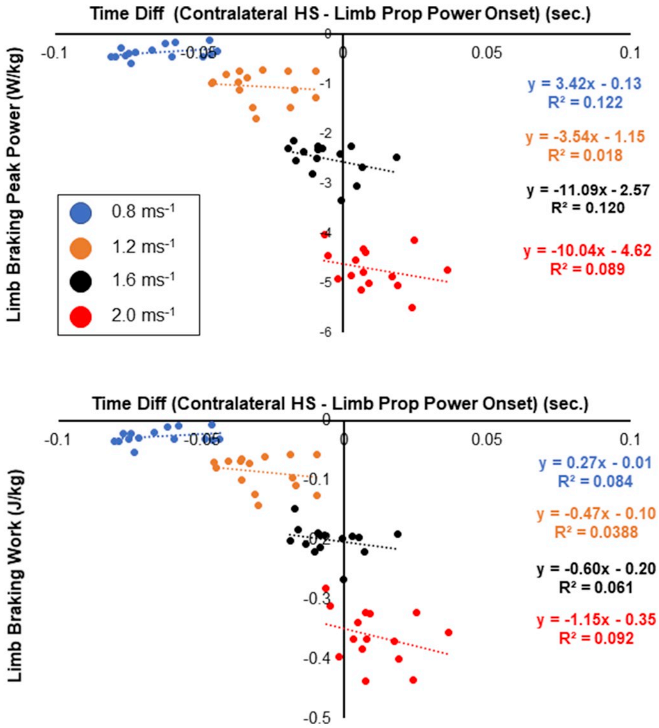

Fig. B1. Top: Relationships between leading limb peak braking power (y-axis) and the time difference between trailing limb propulsion onset (at the limb level) and contralateral heel strike (x-axis). Bottom: Relationships between leading limb braking work (y-axis) and the time difference between trailing limb propulsion onset (at the limb level) and contralateral heel strike (x-axis). Lead limb braking peak power and work are meant to represent collisional losses. Based on the principles of dynamic walking, we expected that individuals who initiated propulsion closer to or before contralateral HS would exhibit lower braking peak power and work from the leading limb (i.e., smaller collisional losses). However, we found no relationship between the timing of propulsion onset and leading limb collisional losses at any of the speeds tested.

References

Adamczyk, P. G., & Kuo, A. D. (2009). Redirection of center-of-mass velocity during the step-to-step transition of human walking. *Journal of Experimental Biology, 212*(16), 2668–2678.

Alexander, N., Strutzenberger, G., Ameshofer, L. M., & Schwameder, H. (2017). Lower limb joint work and joint work contribution during downhill and uphill walking at different inclinations. *Journal of Biomechanics, 61*, 75–80.

Beijersbergen, C. M., Hortobágyi, T., Beurskens, R., Lenzen-Grossimlinghaus, R., Gäbler, M., & Granacher, U. (2016). Effects of power training on mobility and gait biomechanics in old adults with moderate mobility disability: Protocol and design of the potsdam gait study (pogs). *Gerontology, 62*(6), 597–603.

Brandon, L. J., Boyette, L. W., Gaasch, D. A., & Lloyd, A. (2000). Effects of lower extremity strength training on functional mobility in older adults. *Journal of Aging and Physical Activity, 8*(3), 214–227.

Browne, M. G., & Franz, J. R. (2017a). Does dynamic stability govern propulsive force generation in human walking? *Royal Society Open Science, 4*(11), 171673.

Browne, M. G., & Franz, J. R. (2017b). The independent effects of speed and propulsive force on joint power generation in walking. *Journal of Biomechanics, 55*, 48–55.

Burnett, D. R., Campbell-Kyureghyan, N. H., Topp, R. V., & Quesada, P. M. (2015). Biomechanics of lower limbs during walking among candidates for total knee arthroplasty with and without low back pain. *BioMed Research International, 2015*.

Christiansen, C. L., Schenkman, M. L., McFann, K., Wolfe, P., & Kohrt, W. M. (2009). Walking economy in people with parkinson's disease. *Movement Disorders: Official Journal of the Movement Disorder Society, 24*(10), 1481–1487.

Conway, K. A., Bissette, R. G., & Franz, J. R. (2018). The functional utilization of propulsive capacity during human walking. *Journal of Applied Biomechanics, 34*(6), 474–482.

Donelan, J. M., Kram, R., & Kuo, A. D. (2002a). Mechanical work for step-to-step transitions is a major determinant of the metabolic cost of human walking. *Journal of Experimental Biology, 205*(23), 3717–3727.

Donelan, J. M., Kram, R., & Kuo, A. D. (2002b). Simultaneous positive and negative external mechanical work in human walking. *Journal of Biomechanics, 35*(1), 117–124.

Farris, D., & Sawicki, G. S. (2012). The mechanics and energetics of human walking and running: A joint level perspective. *Journal of the Royal Society Interface, 9*(66), 110–118. https://doi.org/10.1098/rsif.2011.0182.

Franz, J. R., & Kram, R. (2014). Advanced age and the mechanics of uphill walking: A joint-level, inverse dynamic analysis. *Gait & Posture, 39*(1), 135–140.

Franz, J. R., Lyddon, N. E., & Kram, R. (2012). Mechanical work performed by the individual legs during uphill and downhill walking. *Journal of Biomechanics, 45*(2), 257–262.

Hurt, C. P., Burgess, J. K., & Brown, D. A. (2015). Limb contribution to increased self-selected walking speeds during body weight support in individuals poststroke. *Gait & Posture, 41*(3), 857–859.

Kadaba, M. P., Ramakrishnan, H., & Wootten, M. (1990). Measurement of lower extremity kinematics during level walking. *Journal of Orthopaedic Research, 8*(3),

383–392.
Kim, C. M., Eng, J. J., MacIntyre, D. L., & Dawson, A. S. (2001). Effects of isokinetic strength training on walking in persons with stroke: A double-blind controlled pilot study. *Journal of Stroke and Cerebrovascular Diseases, 10*(6), 265–273.
Kramer, S., Johnson, L., Bernhardt, J., & Cumming, T. (2016). Energy expenditure and cost during walking after stroke: A systematic review. *Archives of Physical Medicine and Rehabilitation, 97*(4), 619–632 e611.
Kuhman, D., Hammond, K. G., & Hurt, C. P. (2018). Altered joint kinetic strategies of healthy older adults and individuals with parkinson's disease to walk at faster speeds. *Journal of Biomechanics, 79*, 112–118.
Kuo, A. (2001). A simple model of bipedal walking predicts the preferred speed–step length relationship. *Journal of Biomechanical Engineering, 123*(3), 264–269.
Kuo, A. (2002). Energetics of actively powered locomotion using the simplest walking model. *Journal of Biomechanical Engineering, 124*(1), 113–120.
Kuo, A. (2007). The six determinants of gait and the inverted pendulum analogy: A dynamic walking perspective. *Human Movement Science, 26*(4), 617–656.
Kuo, A., & Donelan, M. (2010). Dynamic principles of gait and their clinical implications. *Physical Therapy, 90*(2), 157–174. https://doi.org/10.2522/ptj.20090125.
Lay, A. N., Hass, C. J., & Gregor, R. J. (2006). The effects of sloped surfaces on locomotion: A kinematic and kinetic analysis. *Journal of Biomechanics, 39*(9), 1621–1628.
Malcolm, P., Derave, W., Galle, S., & De Clercq, D. (2013). A simple exoskeleton that assists plantarflexion can reduce the metabolic cost of human walking. *PLoS One, 8*(2), e56137.
Malcolm, P., Quesada, R. E., Caputo, J. M., & Collins, S. H. (2015). The influence of push-off timing in a robotic ankle-foot prosthesis on the energetics and mechanics of walking. *Journal of Neuroengineering and Rehabilitation, 12*(1), 21.
McGeer, T. (1993). Dynamics and control of bipedal locomotion. *Journal of Theoretical Biology, 163*(3), 277–314.
Mian, O. S., Thom, J. M., Ardigò, L. P., Narici, M. V., & Minetti, A. E. (2006). Metabolic cost, mechanical work, and efficiency during walking in young and older men. *Acta Physiologica, 186*(2), 127–139.
Nilsson, J., & Thorstensson, A. (1989). Ground reaction forces at different speeds of human walking and running. *Acta Physiologica Scandinavica, 136*(2), 217–227.
Riley, P. O., Paolini, G., Della Croce, U., Paylo, K. W., & Kerrigan, D. C. (2007). A kinematic and kinetic comparison of overground and treadmill walking in healthy subjects. *Gait & Posture, 26*(1), 17–24.
Ruina, A., Bertram, J. E., & Srinivasan, M. (2005). A collisional model of the energetic cost of support work qualitatively explains leg sequencing in walking and galloping, pseudo-elastic leg behavior in running and the walk-to-run transition. *Journal of Theoretical Biology, 237*(2), 170–192.
Schache, A. G., Brown, N. A., & Pandy, M. G. (2015). Modulation of work and power by the human lower-limb joints with increasing steady-state locomotion speed. *Journal of Experimental Biology, 218*(15), 2472–2481.
Winter, D. A. (1983). Biomechanical motor patterns in normal walking. *Journal of Motor Behavior, 15*(4), 302–330.
Zelik, K. E., & Adamczyk, P. G. (2016). A unified perspective on ankle push-off in human walking. *Journal of Experimental Biology, 219*(23), 3676–3683.
Zelik, K. E., & Kuo, A. D. (2010). Human walking isn't all hard work: Evidence of soft tissue contributions to energy dissipation and return. *Journal of Experimental Biology, 213*(24), 4257–4264.